Published in final edited form as:
*Calcif Tissue Int*. 2011 July ; 89(1): 74–89. doi:10.1007/s00223-011-9496-y.

# Nmp4/CIZ suppresses the response of bone to anabolic parathyroid hormone by regulating both osteoblasts and osteoclasts

**Paul Childress**[1], **Binu K. Philip**[1,§], **Alexander G. Robling**[1,2], **Angela Bruzzaniti**[3], **Melissa A. Kacena**[1,2,4], **Nicoletta Bivi**[1], **Lilian I. Plotkin**[1], **Aaron Heller**[1,†], and **Joseph P. Bidwell**[1,¶]

[1]Department of Anatomy & Cell Biology, Indiana University School of Medicine (IUSM), Indianapolis, IN 46202 USA

[2]Department of Biomedical Engineering, Indiana University-Purdue University at Indianapolis, IN 46202 USA

[3]Department of Oral Biology, Indiana University School of Dentistry, Indianapolis, IN

[4]Department of Orthopaedic Surgery, Indiana University School of Medicine, Indianapolis, IN

## Abstract

How parathyroid hormone (PTH) increases bone mass is unclear but understanding this phenomenon is significant to the improvement of osteoporosis therapy. Nmp4/CIZ is a nucleocytoplasmic shuttling transcriptional repressor that suppresses PTH-induced osteoblast gene expression and hormone-stimulated gains in murine femoral trabecular bone. To further characterize Nmp4/CIZ suppression of hormone-mediated bone growth we treated 10 wk-old *Nmp4*-knockout (KO) and wild-type (WT) mice with intermittent human PTH (1-34) at 30μg/kg/day or vehicle, 7 days/wk, for 2, 3, or 7 wks. Null mice treated with hormone (7 wks) gained more vertebral and tibial cancellous bone than WT animals paralleling the exaggerated response in the femur. Interestingly, Nmp4/CIZ suppression of this hormone-stimulated bone formation was not apparent during the first 2 wks of treatment. Consistent with the null mice enhanced PTH-stimulated addition of trabecular bone these animals exhibited an augmented hormone-induced increase in serum osteocalcin 3 wks into treatment. Unexpectedly the *Nmp4*-KO mice displayed an osteoclast phenotype. Serum C-terminal telopeptides, a marker for bone resorption, was elevated in the null mice, irrespective of treatment. *Nmp4*-KO bone marrow cultures produced more osteoclasts, which exhibited an elevated resorbing activity, compared to WT cultures. The expression of several genes critical to the development of both osteoblasts and osteoclasts were elevated in *Nmp4*-KO mice at 2 wks but not 3 wks of hormone exposure. We propose that Nmp4/CIZ dampens PTH-induced improvement of trabecular bone throughout the skeleton by transiently suppressing hormone-stimulated increases in the expression of proteins key to the required enhanced activity/number of both osteoblasts and osteoclasts.

### Keywords

c-fos; Fra-2; ephrins; osteoclastogenesis; osteocalcin; osteoporosis

¶Address correspondence to: Joseph P. Bidwell, Department of Anatomy & Cell Biology, Indiana University School of Medicine, Medical Science Bldg 5035, 635 Barnhill Drive, Indianapolis, IN 46202, jbidwell@iupui.edu.
§Current address: Bristol-Myers Squibb, Mt.Vernon, IN 47620
†Current address: Kansas City University of Medicine and Biosciences, Kansas City, MO 64106-1453

DISCLOSURES: NONE

## INTRODUCTION

Parathyroid hormone (PTH) therapy is the only osteoporosis treatment that restores bone to the aged skeleton, however its expense makes it the least cost-effective (1, 2). The development of shorter PTH-based treatments yielding similar efficacy as the longer-term therapy will improve its cost-benefit ratio (2) but this requires a better understanding of the mechanisms underlying the PTH anabolic response.

Data on the self-limiting pathways to PTH action, inherent to all endocrine response loops, are lacking and it is these molecules that may provide the best pharmaceutical targets for improving hormone efficacy and cost-effectiveness (3). For example, as PTH activates the osteoblast generation of cAMP and the enhanced expression of RUNX2 it simultaneously stimulates phosphodiesterase activity (4) and Smurf1-mediated RUNX2 proteasomal degradation (5).

We recently demonstrated that disabling the nucleocytoplasmic shuttling transcription factor Nmp4/CIZ (nuclear matrix protein 4/cas interacting zinc finger protein) in mice enhances the skeletal response to anabolic PTH (6) suggestive of a significant role in the hormone's self-limiting pathways. Ten wk-old *Nmp4*-knockout (KO) mice treated with intermittent PTH for 7 wks exhibited an augmented increase in femoral trabecular bone compared to wild-type (WT) mice without compromising the hormone-stimulated increases in bone mineral density and content throughout the skeleton (6).

The ubiquitously expressed Nmp4/CIZ appears to act as a general repressor of anabolic bone growth, in part, by suppressing the transcription of genes that support the development of the osteoblast phenotype, including the pro-alpha1(I) chain (*Col1a1*) and the *Mmp-13* promoters (3, 7, 8). This trans-acting protein suppressed the PTH induction of rat *Mmp-13* transcription in UMR-106-01 osteoblast-like cells via its binding to a PTH-responsive element in the 5′ regulatory region of the gene (8) but whether Nmp4 represses the hormone responsiveness of other tissues has not been reported.

In the present study we determined that Nmp4/CIZ suppressed the PTH-stimulated improvement of trabecular bone throughout the mouse skeleton and was not site-specific as is common in other mouse models (9, 10). Most surprisingly, we discovered that the null mice have an osteoclast phenotype. The analysis of serum biochemistry, bone histomorphometry, bone mRNA expression profiles, and osteoclast cell culture, suggest that the numbers and activities of both osteoblasts and osteoclasts are enhanced in the *Nmp4*-KO mice due, in part, to a transient de-repression of key transcription factors and signaling proteins common to pathways critical for the development and hormone-responsiveness of both cell types.

## MATERIALS AND METHODS

### Mice

Construction of the *Nmp4*-KO mouse, its backcrossing six generations onto a C57BL/6J background, and the baseline phenotype, has been described (6). As in our previous study wild-type C57BL/6J mice from The Jackson Laboratories (Bar Harbor, ME) were used as controls (6). Experiments designed to compare the response of WT and *Nmp4*-KO mice to PTH compensated for any differences in genetic and environmental factors (see Statistical Analyses). Our local Institutional Animal Care and Use Committee approved all experiments and procedures involving the production and use of the experimental mice described in this study.

### PTH treatment regimen

Prior to the start of an experiment 8 wk-old female WT and *Nmp4*-KO mice were given 100μl sterile saline by subcutaneous (sc) injection once daily to acclimatize them to handling. At 10 wks of age, mice were sorted into four groups based on equivalent mean-group-body weight. The four treatment groups included 1) vehicle-treated WT; 2) PTH-treated WT; 3) vehicle-treated *Nmp4*-KO and 4) PTH-treated *Nmp4*-KO. Mice were injected sc with human PTH 1-34 (hPTH(1-34), Bachem Bioscience Inc, PA) at 30μg/kg/day, daily or vehicle control (0.2% BSA/0.1% 1.0 mN HCl in saline, Abbott Laboratory, North Chicago, IL) for the times specified in the Results. Additionally, animals were administered by intraperitoneal injection calcein green (20 mg/kg, Sigma-Aldrich, St Louis, MO) and alizarin red (25 mg/kg, Sigma-Aldrich) 6 days and 3 days before euthanasia, respectively.

### Dual energy x-ray absorptiometry (DEXA)

Bone mineral content (BMC; g), areal bone mineral density (aBMD; mg/cm$^2$), and body weight were measured weekly (8 wks to 12 wks of age). The BMC and aBMD were obtained for the post-cranial skeleton by dual-energy X-ray absorptiometry (DEXA) using an X-ray PIXImus mouse densitometer (PIXImus II; GE-Lunar Corp., Madison, WI) as previously described (6). We report whole body (WB), femur, tibia, and spine BMD and BMC.

### Micro computed tomography (μCT)

Vertebrae, femurs, and tibiae were dissected from the WT and *Nmp4*-KO animals after euthanasia, the connective tissue and muscle removed, and the bones stored in 10% buffered formalin at 4°C. After 48 hr the bones were transferred to 70% ethanol and stored at 4°C until analyzed. We have previously described our methodology for assessing the trabecular microarchitecture at the distal femoral metaphysis and within the 5th lumbar vertebra using the desktop micro-computed μCT 20 tomographer (Scanco Medical AG, Bassersdorf, Switzerland; [6, 9]). Cancellous bone of the tibia was evaluated by scanning the proximal 20% of each tibia at 9 μm resolution. A microfocus X-ray tube with a focal spot of 10 μm was used as a source. Precisely 90 micro-tomograph slices were acquired per bone beginning 1 mm from the epiphysis and extending distally 1.53 mm using a slice increment of 17 μm. For each slice, 600 projections were taken over 216° (180° plus half of the fan angle on either side). Proximal tibia stacks were reconstructed to the 3rd dimension using a standard convolution-backprojection procedure with a Shepp-Logan filter using a threshold value of 275. The Scanco software permitted evaluation of tibial, femoral and vertebral trabecular bone volume per total volume (BV/TV, %), connectivity density (Conn.D, mm$^{-3}$), structure model index (SMI), trabecular number (Tb.N, mm$^{-1}$), trabecular thickness (Tb.Th, mm), and spacing (Tb.Sp, mm) from the 3D constructs. To evaluate cortical architecture, a single slice was taken through the midshaft femur (simply by measuring the number of slices for the whole femur and dividing by 2), and the cortical area (CA, mm$^2$), marrow area (MA, mm$^2$), and the total area (TA, mm$^2$) were calculated (6). Additionally, the moments of inertia, the resistance of the bone to a bending load, were derived from these data. These parameters included the greatest ($I_{MAX}$, mm$^4$) and smallest ($I_{MIN}$, mm$^4$) flexural rigidity as well as the polar moment of inertia (J, mm$^4$), which is the torsional and bending rigidity around the neutral axis of the bone and perpendicular to the x- and y-axes passing through the center of mass (11).

### Quantitative real-time PCR (qRT-PCR) analysis

Femoral or tibial RNA from mice that had been treated with intermittent PTH or vehicle for 2 wks or 3 wks was harvested either 1 hr or 24 hrs after the last injection. The harvesting, processing, and analysis protocols for qRT-PCR analysis have been described (6, 9). Real-

time PCR primers and probes were obtained from Assays-on-Demand™ (Applied Biosystem, Foster City CA, see Table 1). The ΔΔCT method was used to evaluate gene expression between WT and KO animals using *Rplp2* as the normalizer after screening several housekeeping gene candidates. The coefficient of variation of *Rplp2* was typically 2–3% between all samples. Normalization against internal control genes is most frequently used because it can control all variables including cell number (12, 13). The data represent the mean ± standard deviation from at least 6 mice per genotype.

### Bone histomorphometry

Femurs were removed from the WT and *Nmp4*-KO animals after euthanasia and fixed as described above. The anterior face of the epiphyseal plate was cut to expose the marrow cavity. Samples were then dehydrated with graded alcohols, embedded in methyl-methacrylate, sectioned (4μm) with a Leica RM2255 microtome (Leica Microsystems, Wetzlar, Germany), and mounted on standard microscope slides. All histomorphometric parameters were obtained following ASBMR guidelines (14). Mineral apposition rate (MAR), mineralizing surface (MS/BS) and bone formation rate (BFR), were obtained from a $0.03mm^2$ metaphyseal region of interest from 250μm to 1750μm below the growth plate using ImagePro 3.1 software (Media Cybernetics, Bethesda, MD, USA). Some sections were stained for tartarate resistant acid-phosphatase (TRAP). The number of TRAP-positive (TRAP+) cells on the bone surface (TRAP+ cell N/BS) and the TRAP-stained surface to bone surface (TRAP+ S/BS) were determined.

### Serum biochemistry

Intact serum osteocalcin was measured using the sandwich ELISA BTI Mouse Osteocalcin EIA Kit (Biomedical Technologies, Inc., Stoughton MA; [15]). Serum C-terminal telopeptides (CTX) were determined using the RatLaps™ ELISA (Immunodiagnostic Systems Inc., Scottsdale, AZ; [15]).

### Osteoclast culture and activity

To compare the number of osteoclasts derived from *Nmp4*-KO and WT mice, bone marrow was flushed from the long bones of 6–8 week-old animals. Cells were seeded into 24-well culture dishes at an initial density of $2.1\times10^5$ cells/$mm^2$ and cultured in alpha-MEM (Invitrogen, Carlsbad, CA) supplemented with 10% FBS (FBS, Hyclone, Logan Utah) and 20 ng/ml of recombinant human M-CSF (Peprotech, Rocky Hill, NJ) for 2 days and then supplemented with 20 ng/ml of recombinant human M-CSF and 80 ng/ml of recombinant human RANKL (Peprotech) for the duration of the experiment. The cell culture medium was changed every third day until osteoclasts were visible. Once osteoclasts had formed, the cells were fixed with 2.5% glutaraldehyde in phosphate buffered saline for 30 minutes at room temperature, stained for TRAP (Sigma-Aldrich), and TRAP+, multinucleated (≥3) cells were counted.

The osteoclast resorption activity of cells derived from the KO and WT mice was evaluated using a standard pit assay (16). Bone marrow was isolated as above and plated into 6-well culture dishes at $2\times10^6$ cells/well ($2.1\times10^5$ cells/$mm^2$). As detailed above, cells were incubated in alpha-MEM containing 10% FBS and 20 ng/ml M-CSF for 2 days. The media was removed and replaced with fresh media containing 20 ng/ml M-CSF and 80 ng/ml RANKL for an additional 2–3 days. Mature osteoclasts were detached by trypsinization, washed once, re-plated onto dentin slices (Immunodiagnostics Systems Inc, Fountain Hills, AZ) and cultured for an additional 48 hrs in media containing 20 ng/ml M-CSF and 80 ng/ml RANKL. Dentin slices were washed, incubated in 6% NaOCl for 5 min, and sonicated for 20 s to remove cells. Resorption pits were stained with a solution containing 1% toluidine blue and 1% sodium borate for 1 min, washed with water and air-dried. Pit surface

area was quantified using the ImagePro 7.0 on a Leica DMI4000 with a 10X objective. Results were normalized for osteoclast number, as determined by counting TRAP+ cells containing 3 or more nuclei. Experiments were performed in triplicate and results represent average pit area per dentin slice/OC number.

### Statistical analyses

Statistical analysis was processed using JMP Version 7.0.1 (SAS Institute, Cary, NC). Experiments designed to compare the response of WT and *Nmp4*-KO mice to PTH compensated for any differences in genetic and environmental factors, i.e. the fact that WT mice were not bred in-house was accounted for by our analyses. For example, the raw BMD and BMC data were converted to % change (between 8 and 12 wks of age). Comparing hormone-treated to vehicle-treated within each genotype for all the endpoint analyses removed baseline differences from those factors and permitted analysis for genotype × treatment interactions, i.e. whether the WT and *Nmp4*-KO mice responded differently to hormone for the parameter under consideration. We employed a two-factor ANOVA for these analyses. If a genotype × treatment interaction was indicated the data were then analyzed by a Tukey's HSD post hoc test to determine significant differences between the experimental groups. For the serum analysis experiment we used a repeated-measures multivariate analysis of variance (MANOVA) to evaluate the raw longitudinal serum osteocalcin and CTX levels over the 7 wk hormone treatment period. Additionally, we converted the serum data to % change and analyzed with the two-factor ANOVA. The genotype × time term for the raw longitudinal serum data is equivalent to the genotype term for the % change data i.e. both terms indicate a difference in the rate of either osteocalcin/CTX increase or bone accrual (for the BMD/BMC study) between the WT and null mice. For some experiments, unpaired t-tests were employed as indicated. Data are presented as mean ± SD unless otherwise indicated. Statistical significance was taken at $p<0.05$.

## RESULTS

### Nmp4-KO mice exhibited an enhanced PTH-induced acquisition of trabecular bone throughout the skeleton compared to WT mice after 7 wks but not 2 wks of treatment

We previously showed that *Nmp4*-KO mice exhibited a significantly exaggerated PTH-stimulated increase in femoral trabecular bone compared to WT mice after 7 wks of hormone challenge (6); here we addressed whether Nmp4/CIZ represses PTH-induced improvement in other parts of the skeleton and if this suppression is evident from the start of the treatment regimen. Animals were treated with intermittent hPTH(1-34) 30μg/kg/day or vehicle for 7 wks from 10 wks of age. Mice were sorted in the four treatment groups and the cancellous architecture characterized as described in the Material and Methods. The *Nmp4*-KO L5 vertebra BV/TV exhibited a more robust increase in response to 7 wks of PTH than the WT BV/TV as demonstrated by a strong treatment effect and significant genotype × treatment interaction (Figure 1A). The PTH-induced change in vertebral morphology from a rod-like to plate-like form was more pronounced in the null mice (SMI, Figure 1C). Vertebral Tb Th was significantly enhanced in response to 7 wks of hormone in the null mice but not in the WT animals (Figure 1E), whereas PTH had an equivalent impact on Tb Sp (Figure 1F); a consequence of the fact that these parameters do not have a simple reciprocal relationship (14). PTH had an equivalent impact on Conn D (Figure 1B) in the genotypes. Finally, there was a strong genotype effect for all the measured vertebral parameters consistent with the more robust trabecular architecture in the null mice (Figures 1A–1F). Typical μCT scans of L5 vertebra from mice treated with intermittent hormone or vehicle for 7 wks are shown in Figure 1G.

To evaluate the early hormone response of the L5 vertebra we compared bones from WT and *Nmp4*-KO mice that had been treated with PTH or vehicle for 2 wks. The L5 vertebra trabecular bone showed no improvement after 2 wks of hormone in either the WT or null animals (Figure 1A–1F). However, there was a genotype effect for BV/TV, Conn D, SMI, and Tb Th (Figures 1A, 1B, 1C, and 1E, respectively), thus the enhanced vertebral trabecular architecture observed in the 17 wk-old null mice irrespective of treatment, was apparent in these mice at 12 wks of age.

Nmp4/CIZ also repressed the hormone-induced increase in tibial cancellous bone (Figure 2). The PTH-stimulated increase in tibial BV/TV after 7 wks of hormone was greater in the null than the WT mice (Figure 2A). PTH increased tibial Tb N in both genotypes but significantly more so in the null mice (Figure 2D) and the hormone-stimulated change in tibial SMI was more pronounced in the null mice (Figure 2C). PTH had a comparable positive effect on Conn D (Figure 2B), Tb Th, (Figure 2E), and Tb Sp (Figure 2F) in the WT and null mice with 7 wks of treatment. Typical μCT scans of tibia from mice treated with hormone or vehicle for 7 wks are shown in Figure 2G.

To evaluate the early hormone response of the tibia we compared bones from WT and *Nmp4*-KO mice that had been treated with PTH or vehicle for 2 wks. Both genotypes showed equal hormone-induced improvement of tibial BV/TV, Conn D, SMI, and Tb Th during the initial 2 wks of treatment (Figures 2A, 2B, 2C, 2E). PTH failed to improve Tb N and Tb Sp in both WT and null mice during this period of the regimen, however there was a genotype effect for these two parameters indicating enhanced aspects of tibial architecture in the null mice at 12 wks of age (Figure 2D & 2F).

Disabling Nmp4 had no impact on any aspect of the skeletal response to PTH (no genotype × treatment interaction) during the first 2 wks of treatment including femoral cancellous architecture (Table 2A), midshaft cortical architecture (Table 2B) and the percent change skeletal BMD and BMC (Table 2C). Consistent with Nmp4 repressive action on bone growth (6) genotype effects were observed for some of these parameters indicative of the modestly enhanced skeletal phenotype of the null animals. Interestingly, the genotype effects for WB BMC and femur and tibia BMD and BMC (Table 2C) indicated that the rate of bone accrual was lower in the null mice over the four-week period of measurement irrespective of treatment.

### The enhanced PTH-stimulated increase in femoral trabecular bone observed in Nmp4-KO mice occurred after 2 wks and before 7 wks of hormone exposure

Histological sections of the femoral spongiosa prepared for histomorphometry (Figure 3A) confirmed our previous analysis using μCT (6) that the *Nmp4*-KO mice added more cancellous bone in response to 7 wks of hormone treatment than WT mice. However, bone formation rate parameters were not different between the null and WT mice at the end of treatment and in fact were declining suggesting that PTH response was beginning to plateau in both genotypes. MS/BS, *proportion of bone surface undergoing mineralization*, was significantly decreased in both genotype treatment groups consistent with the declining PTH-responsiveness (Table 2D). Additionally, we did not observe a significant hormone-induced increase in bone formation rate (BFR) in either of the genotypes at this point in treatment (Table 2D). Nevertheless, PTH equally enhanced the mineral apposition rate (MAR) in both genotypes at this time point (Table 2D).

Our histomorphometric analysis of mice treated with PTH or vehicle for 7 wks included the parameters of TRAP+ S/BS and TRAP+ N/BS, which provide an estimate of the size and number of osteoclast precursors and mature osteoclasts normalized to bone surface. Clearly the anabolic hormone treatment enhanced the absolute number of osteoclasts and the total

osteoclast surface over bone in both genotypes as evident from the histological sections (Figure 3B); normalizing these parameters to bone surface reveals that although both parameters are elevated in the null mice the differences are not statistically significant (Table 2D). However there were strong treatment effects, i.e. PTH significantly attenuated the percent bone surface covered by TRAP+ cells and their number/surface (Table 2D). Interestingly there was a genotype × treatment interaction for TRAP+ S/BS indicating that hormone had a larger impact on the reduction of bone surface covered by osteoclasts in the null mice than in the WT animals (Table 2D).

## Nmp4-KO mice exhibited strikingly different serum osteocalcin and CTX profiles compared to WT animals

Whole blood was collected and serum separated from the mice of the four treatment groups at 10 wks of age (before initiation of treatment), 13 wks of age (3 wks of PTH/vehicle treatment), and 17 wks of age (7 wks of PTH/vehicle treatment). The raw longitudinal data and the % change data for osteocalcin, a standard marker for bone formation and osteoblast number, revealed that null and WT mice had equivalent serum levels just prior to hormone treatment but the *Nmp4*-KO mice exhibited a higher rate of increase over the hormone treatment period (genotype × time interaction, longitudinal data; genotype interaction, % change data) and exhibited an enhanced response to hormone (genotype × treatment interaction, Figures 4A & 4B). Specifically, the null mice showed an enhanced and sustained increase in osteocalcin after 3 wks of treatment while the WT animals showed a peak at 3 wks of treatment followed by a decline by 7 wks of treatment (Figure 4A & 4B).

Serum C-terminal telopeptides (CTX), a marker for bone resorption, was significantly elevated in the *Nmp4*-KO mice compared to the WT animals before and during the hormone treatment period. CTX was elevated with PTH treatment in both genotypes but this increase was not statistically significant (Figure 4C & 4D).

## Bone marrow from Nmp4-KO mice yields more osteoclasts than marrow from WT mice and the null osteoclasts exhibit an enhanced resorbing activity

To confirm our serum data indicating an increased activity of osteoclasts in the *Nmp4*-KO mice we compared the number of these cells derived from the bone marrow cultures of the untreated null and WT animals at 7–8 wks of age. Bone marrow preparations from 3 null mice and 4 WT mice were cultured in 6-well plates and treated with M-CSF and RANKL as described in the Materials and Methods section. On average, the *Nmp4*-KO bone marrow cultures produced 2-fold more osteoclasts than the WT marrow (null = 1608 ± 87 OC/well; WT = 877 ± 243 OC/well; $p<0.05$, data presented as average ± SD). This experiment was performed twice yielding similar results.

Next we compared the dentin-resorbing activities of the *Nmp4*-KO and WT osteoclasts. Mature osteoclasts were obtained from the bone marrow of WT and null mice (n=2–3 mice per group) as described in the Materials and Methods section. Fully differentiated bone marrow-derived osteoclasts were re-plated on dentin slices for 48 hrs. The area resorbed was quantified and normalized for TRAP+ osteoclasts. The *Nmp4*-KO osteoclasts exhibited a 50% increase in the area resorbed on dentin compared to the WT osteoclasts (null = 154 ± 4.6 % area resorbed/Trap+ cells; WT = 100 ± 13.3 % area resorbed/Trap+ cells; $p<0.05$, data presented as average ± SD).

## Nmp4-KO mice exhibit a transiently enhanced basal or PTH-stimulated expression of genes common to osteoblast and osteoclast development

To follow up on our observation that both osteoblast and osteoclast numbers were enhanced in the null mice, we analyzed femoral RNA harvested during the early phase of PTH

treatment to evaluate the expression of genes that support the development of both cells. Animals were treated with intermittent PTH or vehicle for 2 or 3 wks and RNA harvested 1 hr after the last injection. The AP-1 transcription factors *c-fos* and *Fra-2* both exhibited a significantly enhanced PTH-stimulated increase in the *Nmp4*-KO mice (genotype × treatment interaction) after 2 wks of treatment but these differences were absent after 3 wks of PTH (Table 3A). Additionally, the transcription factor *Nfatc1* was significantly elevated in the femur of null mice (genotype effect) at the 2 wk time point but was equivalent to the WT expression at 3 wks of treatment (Table 3A). We also examined the expression of several genes that mediate osteoblast-osteoclast signaling. Interestingly, the *Nmp4*-KO mice showed a significant increase in the expression of *EphB4* the receptor for *EphrinB2*, its transmembrane ligand, which also showed an elevation in expression that approached significance but again these differences between the genotypes disappeared at the 3 wk time point (Table 3A). Both EphB4 and EphrinB2 were responsive to PTH in the null and WT mice (Table 3A). Interestingly, the *Rankl/Opg* ratio was diminished in the null mice compared to WT animals at 2 and 3 wks of treatment, which was significant at the latter time point (Figure 3A).

Further comparative analysis of femoral gene expression profiles between WT and null mice at the 2 wk time period failed to show any significant differences between the two genotypes with one exception (Table 3B). The expression of the pro-survival gene *Bcl2* was not different in WT and null mice and did not respond to hormone in either genotype at this point in the treatment regimen, however, the expression of *Bax*, the pro-apoptotic gene was significantly attenuated in the *Nmp4*-KO mice (Table 3B). *M-csf*, its receptor *c-fms*, and the osteoclast recruitment cytokine *Mcp-1* showed no difference in their expression or PTH-responsiveness between WT and *Nmp4*-KO animals (Table 3B). Hormone induced over a 25-fold increase in *Nurr1* expression in both WT and null mice (Table 3B). The expressions of *Mkp-1*, *JunD*, *Smad3*, and *Lef1* were modestly but equally elevated with PTH in both genotypes (Table 3B). Conversely, the mRNA expression of the receptor for advanced glycation end products (*Rage*) was attenuated by hormone treatment in both WT and *Nmp4*-KO mice (Table 3B).

Next we characterized the expression of genes that support bone formation by analyzing femoral RNA obtained 24 hr after the last injection of intermittent PTH or vehicle after 2 wks of treatment. We observed a treatment effect, but no genotype effect or genotype × treatment interaction for *Runx2*, *Osterix*, *Col1a1*, *Alpl* and *Mmp13*, *Sost*, *Bmp2*, *and Pthr1* mRNA profiles (Table 3B). Intermittent hormone treatment did not impact the expression of PTH-related peptide (*Pthrp*) in either genotype (Table 3B).

Our preliminary evaluation of gene expression in the tibia showed that the RNA profiles at 3 wks of treatment were generally similar to those observed for the femur at the same time point with the exception of *Nfatc1*, which was still significantly elevated in the tibia of the null mice (Table 3C). Additionally, the decrease in the *Rankl/Opg* ratio did not reach significance in the tibia as demonstrated for the femur (Table 3C).

## DISCUSSION

The present data demonstrate that Nmp4/CIZ significantly blunts PTH-stimulated improvement in cancellous bone throughout the skeleton, that this repression of bone gain is apparent between 2 wks and 7 wks of hormone treatment, and that Nmp4/CIZ suppresses osteoclast as well as osteoblast number and activity likely by regulating key transcription factors critical to the development of both cells. The global impact of Nmp4 on the trabecular skeleton is in stark contrast to recent studies showing the site-specific effects of Rage (9) and connexin 43 (10) on PTH-induced cancellous bone improvement.

Nmp4/CIZ repression of the PTH-mediated increase in trabecular bone was not observed during the initial 2 wk treatment period; WT and KO mice showed equivalent hormone-stimulated increases in BMD, BMC, trabecular improvement, and enhanced expression of numerous genes that support bone formation. At 7 wks of hormone challenge the striking expansion of the null trabecular compartment had been added and bone histomorphometry indicated that both the KO and WT mice exhibited a diminished response to PTH consistent with previous observations on C57BL/6 mice (17). However, starting at 3 wks of hormone challenge the KO mice exhibited an enhanced and sustained PTH-induced increase in serum osteocalcin. The significance of the 2–3 wk lag period required for distinguishing the difference in PTH-stimulated bone formation between the *Nmp4*-KO and WT mice remains to be elucidated. Does this delay represent the time necessary to dramatically expand the null bone-forming osteoblast population? Further histomorphometric analysis at various time points throughout the treatment regimen is required to address this question.

Of particular significance was our discovery of an osteoclast phenotype in the *Nmp4*-KO mouse. The null mice had significantly higher serum CTX; more osteoclasts were recovered from *Nmp4*-KO marrow cultures than from WT cultures, and the null osteoclasts were more active as determined by in vitro resorption of dentin. Interestingly, PTH had a more significant impact on decreasing the osteoclast-covered bone surface in null mice without significantly lowering serum CTX, perhaps in part a consequence of the enhanced activity of the null osteoclasts. Despite the multiple lines of evidence suggesting higher bone resorption in the untreated nulls these mice are not osteopenic and in fact have a modestly enhanced skeleton, although the rate of bone accrual from 8–12 wks is marginally slower in the null animals. Femoral bone marrow-derived osteoblasts from Nmp4/CIZ-deficient mice exhibited an enhanced alkaline phosphatase expression and formed more mineralized nodules than wild-type osteoblasts (18), suggesting in vivo that the null osteoblast outpaces the null osteoclast. Further study is required to determine if there is an increased rate of remodeling (activation frequency) with a positive bone balance in the untreated mice and if so, how this is achieved.

Although the in vivo mRNA expression profiles represent a composite of multiple marrow and bone cell types, the transiently enhanced expression of *c-fos*, *Fra-2*, and *Nfatc1* in the null mice may be part of the molecular mechanism contributing to the apparent increased number of osteoblasts and osteoclasts. Fra-2 plays a significant role in chondrocyte differentiation and matrix production in embryonic and newborn mice (19) and in regulating the size of osteoclasts (20).

The contribution of c-Fos to the PTH anabolic response involves both osteoblasts and osteoclasts; in the former it is part of the immediate-early gene response (21) and as such is critical for subsequent induction of select target genes. As a key regulator of bone cell growth and differentiation, c-Fos often interacts with RUNX2 (22). PTH stimulation of *Mmp-13* transcription in osteoblast-like cells requires the cooperative interaction between the c-Fos•c-Jun AP-1 complex and RUNX2 (23), and Nmp4/CIZ dampens this induction (8). Consequently, the heightened PTH-stimulated increase in osteoblast c-Fos activity in the *Nmp4*-KO mice may boost hormone transcriptional induction of some genes supporting the anabolic response. The impact of Nmp4/CIZ on *c-fos* and *Fra-2* was specific within the context of the PTH-induce immediate-early response because we did not observe differences in other aspects of this gene program including *Nurr1*, a transcription factor participating in PTH-mediated osteoblast gene induction (24), *Mkp-1*, a phosphatase implicated in PTH-mediated osteoblast cell cycle arrest (25), *JunD*, involved in osteoblast differentiation (26), or *Smad3* and *Lef1*, trans-acting proteins involved in coupling the PTH and Wnt signaling pathways in osteoblasts (27).

In addition to its role as a PTH-responsive osteoblast transcription factor c-Fos is critical to osteoclastogenesis and plays a role in supporting the precursor cell's capacity to undergo differentiation (28). It fulfills this role in part by mediating the induction of *Nfatc1*, another key transcription factor that supports osteoclastogenesis and osteoblast development (29); the elevation of *c-fos* mRNA expression in the nulls may ultimately contribute to the enhanced *Nfatc1* expression in these mice. Additionally, c-Fos has multiple and complex roles in regulating osteoblast-derived signals that regulate osteoclastogenesis and mature osteoclast activity including the RANKL/OPG signaling axis by governing the transcriptional activity of the *Opg* gene in the osteoblast and by activating RANKL target genes in osteoclasts; c-Fos also activates the IFN-gamma-driven RANKL negative feedback pathway in the osteoclast (30, 31). The *Rankl/Opg* ratio was attenuated in the null mice, which achieved significance in the femur by 3 wks of treatment; perhaps this ultimately contributed some protective effect from the enhanced osteoclast activity. Nmp4/CIZ had negligible impact on the mRNA expression of other osteoclastogenic cytokines including *Mcp-1*, a cytokine involved in osteoclast recruitment (32), *M-csf* and its receptor *c-fms* that activate the proliferation and survival of osteoclast precursors (33). The significantly attenuated expression of the pro-apoptotic gene, Bax, in the null mice may contribute to a longer-lived osteoblast, critical to the PTH-induced anabolic mechanism (5), but further studies are required to confirm this possibility.

Recent studies with *c-fos*-null animals indicate that interaction between immature osteoclasts and pre-osteoblasts may be necessary for an optimal response to intermittent PTH; specifically the osteoclast precursors support the differentiation of pre-osteoblasts (34, 35; 36). In one potential scenario this coupling is mediated by the bidirectional interaction between an EphrinB2 ligand on the pre-osteoclast and the EphB4 receptor on the pre-osteoblast (34, 35). Forward signaling from the osteoclast precursor to the pre-osteoblast enhances differentiation of the latter whereas reverse signaling suppresses osteoclast differentiation (35). Therefore, PTH appears to activate both forward and reverse EphrinB-EphB4 signaling resulting in the enhancement of bone formation and the restraining of resorption (34). This is consistent with the observed increased expression of EphB4 in the *Nmp4*-KO mice and the marginally enhanced ephrinB2 expression in these animals. Future osteoblast-osteoclast co-culture studies will be needed to investigate the potential impact of Nmp4/CIZ on the reciprocal regulation of these cells.

We propose that Nmp4/CIZ governs both the osteoblast and osteoclast cellular arms of the PTH-induced anabolic response by controlling the size, activity, and/or PTH-responsiveness of these cell populations in part via the modest suppression of several key transcription factors and receptors critical to the developmental and/or response pathways of both cells. The complex sequence of molecular and cellular events underlying Nmp4/CIZ regulation of bone remodeling remains to be elucidated. Nmp4/CIZ has been previously identified as an attractive potential therapeutic target for treating osteoporosis (37), and the present finding that this protein not only regulates the osteoblast but also the osteoclast underscores this assertion.

## Acknowledgments

This work was supported by a grant from NIH NATIONAL INSTITUTE OF DIABETES AND DIGESTIVE AND KIDNEY DISEASES (NIDDK), contract grant number DK053796 (JPB).

## References

1. Stroup J, Kane MP, Abu-Baker AM. Teriparatide in the treatment of osteoporosis. Am J Health Syst Pharm. 2008; 65:532–539. [PubMed: 18319498]

2. Liu H, Michaud K, Nayak S, Karpf DB, Owens DK, Garber AM. The cost-effectiveness of therapy with teriparatide and alendronate in women with severe osteoporosis. Arch Intern Med. 2006; 166:1209–1217. [PubMed: 16772249]

3. Childress P, Robling AG, Bidwell JP. Nmp4/CIZ: road block at the intersection of PTH and load. Bone. 2010; 46:259–266. [PubMed: 19766748]

4. Ahlström M, Lamberg-Allardt C. Rapid protein kinase A-mediated activation of cyclic AMP-phosphodiesterase by parathyroid hormone in UMR-106 osteoblast-like cells. J Bone Miner Res. 1997; 12:172–8. [PubMed: 9041048]

5. Bellido T, Ali AA, Plotkin LI, Fu Q, Gubrij I, Roberson PK, Weinstein RS, O'Brien CA, Manolagas SC, Jilka RL. Proteasomal degradation of Runx2 shortens parathyroid hormone-induced anti-apoptotic signaling in osteoblasts. A putative explanation for why intermittent administration is needed for bone anabolism. J Biol Chem. 2003; 278:50259–50272. [PubMed: 14523023]

6. Robling AG, Childress P, Yu J, Cotte J, Heller A, Philip BK, Bidwell JP. Nmp4/CIZ suppresses parathyroid hormone-induced increases in trabecular bone. J Cell Physiol. 2009

7. Thunyakitpisal P, Alvarez M, Tokunaga K, Onyia JE, Hock J, Ohashi N, Feister H, Rhodes SJ, Bidwell JP. Cloning and functional analysis of a family of nuclear matrix transcription factors (NP/NMP4) that regulate type I collagen expression in osteoblasts. J Bone Miner Res. 2001; 16:10–23. [PubMed: 11149472]

8. Shah R, Alvarez M, Jones DR, Torrungruang K, Watt AJ, Selvamurugan N, Partridge NC, Quinn CO, Pavalko FM, Rhodes SJ, Bidwell JP. Nmp4/CIZ regulation of matrix metalloproteinase 13 (MMP-13) response to parathyroid hormone in osteoblasts. Am J Physiol Endocrinol Metab. 2004; 287:E289–96. [PubMed: 15026307]

9. Philip BK, Childress PJ, Robling AG, Heller A, Nawroth PP, Bierhaus A, Bidwell JP. RAGE supports parathyroid hormone-induced gains in femoral trabecular bone. Am J Physiol Endocrinol Metab. 2010; 298:E714–E725. [PubMed: 20028966]

10. Chung DJ, Castro CH, Watkins M, Stains JP, Chung MY, Szejnfeld VL, Willecke K, Theis M, Civitelli R. Low peak bone mass and attenuated anabolic response to parathyroid hormone in mice with an osteoblast-specific deletion of connexin43. J Cell Sci. 2006; 119:4187–4198. [PubMed: 16984976]

11. Cheng S, Sipilä S, Taaffe DR, Puolakka J, Suominen H. Change in bone mass distribution induced by hormone replacement therapy and high-impact physical exercise in post-menopausal women. Bone. 2002; 31:126–135. [PubMed: 12110425]

12. Goossens K, Van Poucke M, Van Soom A, Vandesompele J, Van Zeveren A, Peelman LJ. Selection of reference genes for quantitative real-time PCR in bovine preimplantation embryos. BMC Dev Biol. 2005:5–27. [PubMed: 15725348]

13. Zhang X, Ding L, Sandford AJ. Selection of reference genes for gene expression studies in human neutrophils by real-time PCR. BMC Mol Biol. 2005; 6:4. [PubMed: 15720708]

14. Parfitt AM, Drezner MK, Glorieux FH, Kanis JA, Malluche H, Meunier PJ, Ott SM, Recker RR. Bone histomorphometry: standardization of nomenclature, symbols, and units. Report of the ASBMR Histomorphometry Nomenclature Committee. J Bone Miner Res. 1987; 2:595–610. [PubMed: 3455637]

15. O'Brien CA, Plotkin LI, Galli C, Goellner JJ, Gortazar AR, Allen MR, Robling AG, Bouxsein M, Schipani E, Turner CH, Jilka RL, Weinstein RS, Manolagas SC, Bellido T. Control of bone mass and remodeling by PTH receptor signaling in osteocytes. PLoS One. 2008; 3:e2942. [PubMed: 18698360]

16. Tanaka S, Amling M, Neff L, Peyman A, Uhlmann E, Levy JB, Baron R. c-Cbl is downstream of c-Src in a signalling pathway necessary for bone resorption. Nature. 1996; 383:528–531. [PubMed: 8849724]

17. Iida-Klein A, Zhou H, Lu SS, Levine LR, Ducayen-Knowles M, Dempster DW, Nieves J, Lindsay R. Anabolic action of parathyroid hormone is skeletal site specific at the tissue and cellular levels in mice. J Bone Miner Res. 2002; 17:808–816. [PubMed: 12009011]

18. Morinobu M, Nakamoto T, Hino K, Tsuji K, Shen ZJ, Nakashima K, Nifuji A, Yamamoto H, Hirai H, Noda M. The nucleocytoplasmic shuttling protein CIZ reduces adult bone mass by inhibiting

bone morphogenetic protein-induced bone formation. J Exp Med. 2005; 201:961–970. [PubMed: 15781586]

19. Karreth F, Hoebertz A, Scheuch H, Eferl R, Wagner EF. The AP1 transcription factor Fra2 is required for efficient cartilage development. Development. 2004; 131:5717–25. [PubMed: 15509771]
20. Bozec A, Bakiri L, Hoebertz A, Eferl R, Schilling AF, Komnenovic V, Scheuch H, Priemel M, Stewart CL, Amling M, Wagner EF. Osteoclast size is controlled by Fra-2 through LIF/LIF-receptor signalling and hypoxia. Nature. 2008; 454:221–5. [PubMed: 18548006]
21. Liang JD, Hock JM, Sandusky GE, Santerre RF, Onyia JE. Immunohistochemical localization of selected early response genes expressed in trabecular bone of young rats given hPTH 1-34. Calcif Tissue Int. 1999; 65:369–373. [PubMed: 10541762]
22. Qin L, Raggatt LJ, Partridge NC. Parathyroid hormone: a double-edged sword for bone metabolism. Trends Endocrinol Metab. 2004; 15:60–65. [PubMed: 15036251]
23. D'Alonzo RC, Selvamurugan N, Karsenty G, Partridge NC. Physical interaction of the activator protein-1 factors c-Fos and c-Jun with Cbfa1 for collagenase-3 promoter activation. J Biol Chem. 2002; 277:816–822. [PubMed: 11641401]
24. Nervina JM, Magyar CE, Pirih FQ, Tetradis S. PGC-1alpha is induced by parathyroid hormone and coactivates Nurr1-mediated promoter activity in osteoblasts. Bone. 2006; 39:1018–25. [PubMed: 16765661]
25. Qin L, Li X, Ko JK, Partridge NC. Parathyroid hormone uses multiple mechanisms to arrest the cell cycle progression of osteoblastic cells from G1 to S phase. J Biol Chem. 2005; 280:3104–11. [PubMed: 15513917]
26. Wagner EF. Bone development and inflammatory disease is regulated by AP-1 (Fos/Jun). Ann Rheum Dis. 2010; 69(Suppl 1):i86–88. [PubMed: 19995753]
27. Tobimatsu T, Kaji H, Sowa H, Naito J, Canaff L, Hendy GN, Sugimoto T, Chihara K. Parathyroid hormone increases beta-catenin levels through Smad3 in mouse osteoblastic cells. Endocrinology. 2006; 147(5):2583–2590. [PubMed: 16484320]
28. Boyle WJ, Simonet WS, Lacey DL. Osteoclast differentiation and activation. Nature. 2003; 423:337–342. [PubMed: 12748652]
29. Takayanagi H. The role of NFAT in osteoclast formation. Ann N Y Acad Sci. 2007; 1116:227–237. [PubMed: 18083930]
30. Takayanagi H, Kim S, Matsuo K, Suzuki H, Suzuki T, Sato K, Yokochi T, Oda H, Nakamura K, Ida N, Wagner EF, Taniguchi T. RANKL maintains bone homeostasis through c-fos-dependent induction of interferon-beta. Nature. 2002; 416:744–749. [PubMed: 11961557]
31. Fu Q, Jilka RL, Manolagas SC, O'Brien CA. Parathyroid hormone stimulates receptor activator of NFkappa B ligand and inhibits osteoprotegerin expression via protein kinase A activation of cAMP-response element-binding protein. J Biol Chem. 2002; 277:48868–48875. [PubMed: 12364326]
32. Li X, Qin L, Bergenstock M, Bevelock LM, Novack DV, Partridge NC. Parathyroid hormone stimulates osteoblastic expression of MCP-1 to recruit and increase the fusion of pre/osteoclasts. J Biol Chem. 2007; 282:33098–106. [PubMed: 17690108]
33. Negishi-Koga T, Takayanagi H. Ca2+-NFATc1 signaling is an essential axis of osteoclast differentiation. Immunol Rev. 2009; 231:241–256. [PubMed: 19754901]
34. Luiz de Freitas PH, Li M, Ninomiya T, Nakamura M, Ubaidus S, Oda K, Udagawa N, Maeda T, Takagi R, Amizuka N. Intermittent PTH administration stimulates pre-osteoblastic proliferation without leading to enhanced bone formation in osteoclast-less c-fos(−/−) mice. J Bone Miner Res. 2009; 24:1586–1597. [PubMed: 19419301]
35. Zhao C, Irie N, Takada Y, Shimoda K, Miyamoto T, Nishiwaki T, Suda T, Matsuo K. Bidirectional ephrinB2-EphB4 signaling controls bone homeostasis. Cell Metab. 2006; 4:111–121. [PubMed: 16890539]
36. Koh AJ, Demiralp B, Neiva KG, Hooten J, Nohutcu RM, Shim H, Datta NS, Taichman RS, McCauley LK. Cells of the osteoclast lineage as mediators of the anabolic actions of parathyroid hormone in bone. Endocrinology. 2005; 146(11):4584–4596. [PubMed: 16081645] Allen MR,

Burr DB. Parathyroid hormone and bone biomechanics Clinical Reviews in Bone and Mineral Metabolism. 2006; 4:259–68.

37. Krane SM. Identifying genes that regulate bone remodeling as potential therapeutic targets. J Exp Med. 2005; 201:841–843. [PubMed: 15781576]

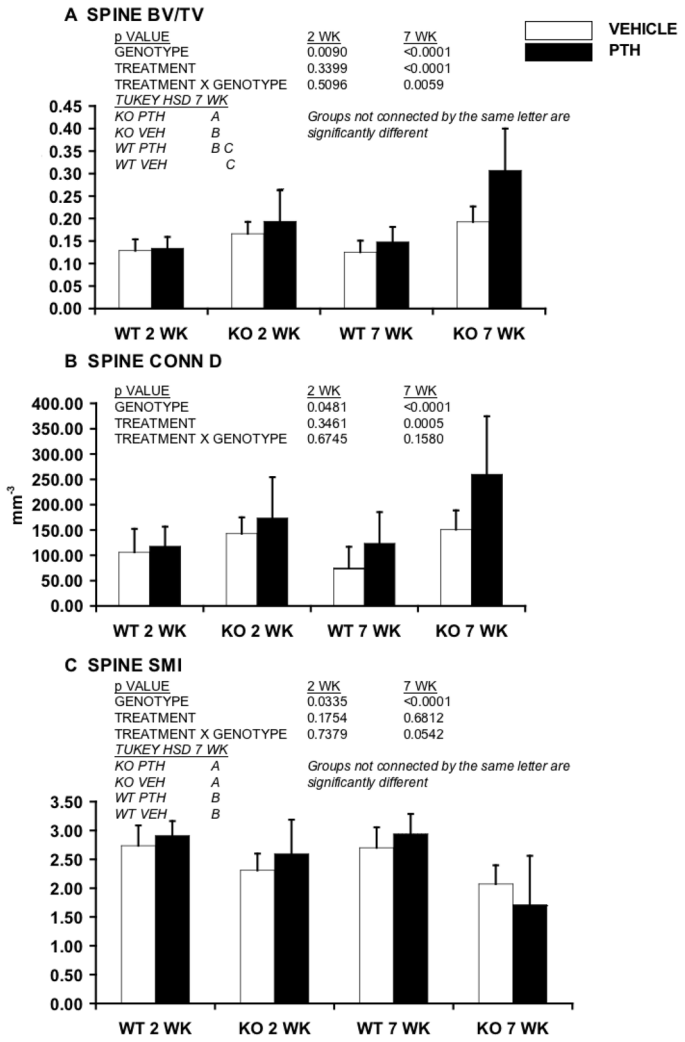

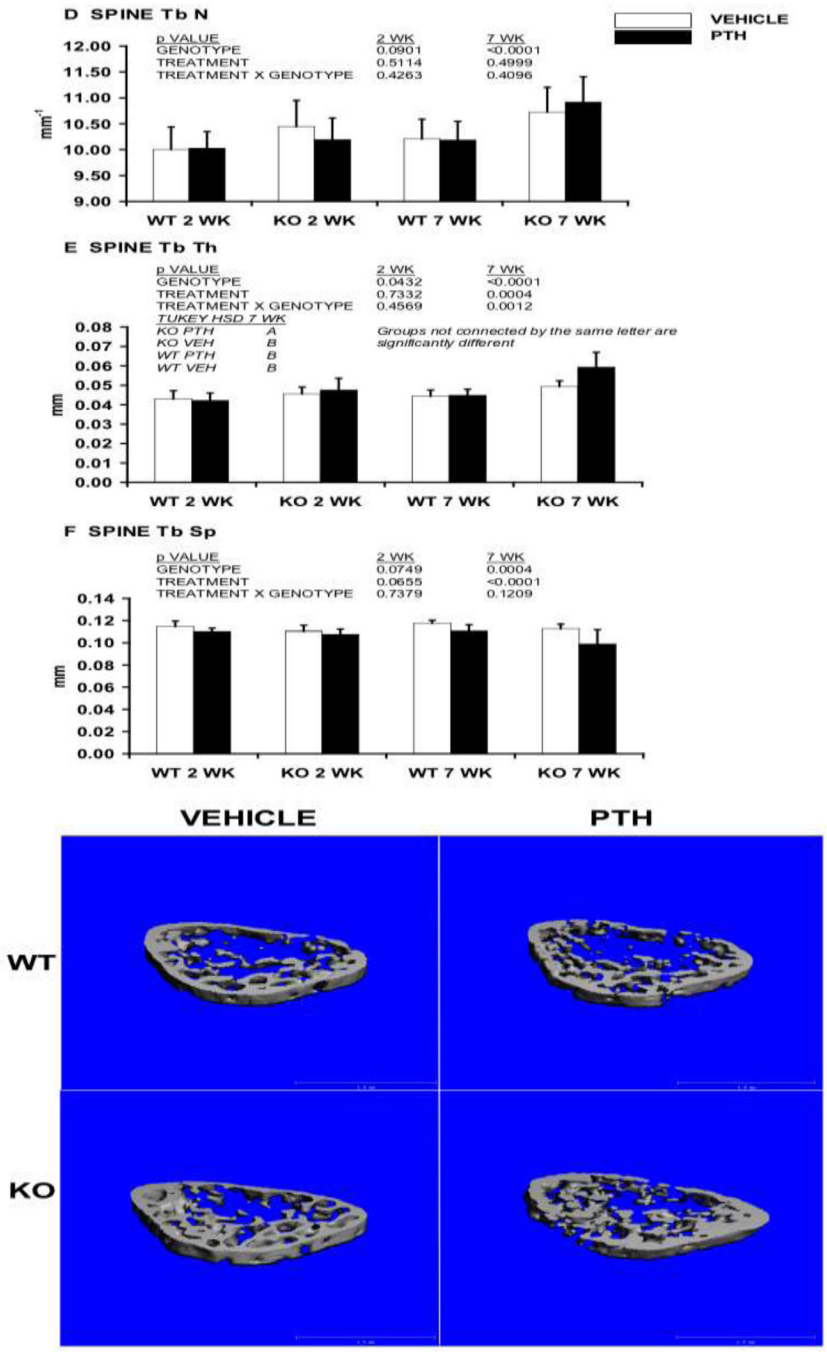


**Figure 1.**

Disabling Nmp4 enhanced PTH responsiveness of vertebral cancellous bone. Micro-CT-acquired vertebral (L5) trabecular architecture including (A) BV/TV, %; (B) Conn D, $mm^{-3}$; (C) SMI, (D) Tb N $mm^{-1}$, (E) Tb Th mm, (F) Tb Sp mm was compared between WT and *Nmp4*-KO mice that had been treated with intermittent hPTH(1-34) 30μg/kg/day or vehicle for 7 wks (number of mice/experimental group=11–12). To evaluate the early hormone response we compared bones from WT and *Nmp4*-KO mice that had been treated with intermittent PTH or vehicle for 2 wks using the same experimental design (number of mice/experimental group=5–7). No improvement was observed after 2 wks of intermittent

PTH treatment in either the WT or null animals (A–F). There was a genotype effect for BV/TV, Conn D, SMI, and Tb Th (A, B, C, and E, respectively) consistent with the enhanced trabecular architecture of the null mice, regardless of treatment. (G) μCT images of vertebral trabecular bone from WT and *Nmp4*-KO mice that had been treated with intermittent PTH or vehicle for 7 wks, Scale bar=1mm. Data is presented as average ± SD. The listed p-values were determined with a two-factor ANOVA. A Tukey's HSD post hoc test was used to determine differences between the treatment groups if a significant genotype × treatment interaction was indicated.

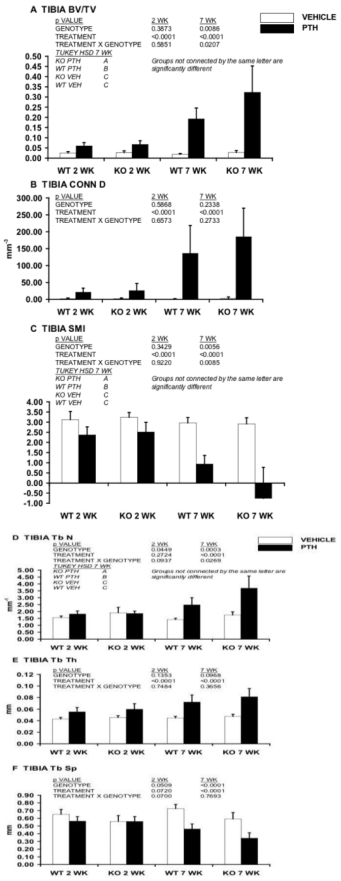


**Figure 2.**

*Nmp4*-KO mice exhibited an enhanced PTH-induced increase in tibial trabecular bone. Micro-CT-acquired tibial trabecular architecture including (A) BV/TV, %; (B) Conn D, mm-3; (C) SMI, (D) Tb N mm-1, (E) Tb Th mm, (F) Tb Sp mm was compared between WT and *Nmp4*-KO mice that had been treated with intermittent PTH or vehicle for 7 wks (number of mice/experimental group=8). To evaluate the early hormone response we compared bones from WT and *Nmp4*-KO mice that had been treated with intermittent PTH or vehicle for 2 wks (number of mice/experimental group=7–9). Both genotypes showed equal hormone-induced improvement of tibial (A) BV/TV, (B) Conn D, (C) SMI, and (E) Tb Th during the initial 2 wks of treatment. There was a genotype effect for (D) Tb N and (F) Tb Sp indicating enhanced aspects of tibial architecture in the null mice at 12 wks of age irrespective of treatment. (G) μCT images of tibial trabecular bone from WT and *Nmp4*-KO mice that had been treated with intermittent PTH or vehicle for 7 wks, Scale bar=1mm. The listed p-values were determined with a two-factor ANOVA. A Tukey's HSD post hoc test was used to determine differences between the treatment groups if a significant genotype × treatment interaction was indicated.

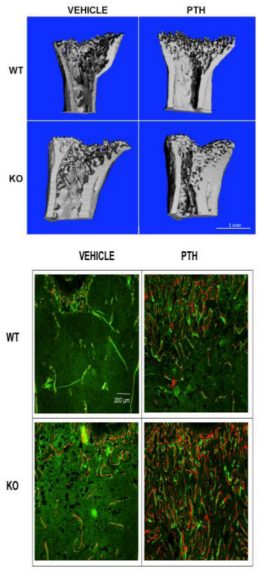


**Figure 3.**

[A] PTH-induced improvements in femoral trabecular architecture were enhanced in *Nmp4*-KO mice, after 7 wks of treatment. The femoral tissue sections were obtained from WT and *Nmp4*-KO mice treated with intermittent PTH or vehicle for 7 wks (number of mice/experimental group=5–6). Additionally, animals were administered by intraperitoneal injection calcein green (20mg/kg) and alizarin red (25mg/kg) 6 days and 3 days before euthanasia, respectively. [B] Sections were stained for tartarate resistant acid-phosphatase (TRAP) to evaluate osteoclast number and surface. Histological sections were prepared as described in the Materials and Methods. Scale bar=200 μm

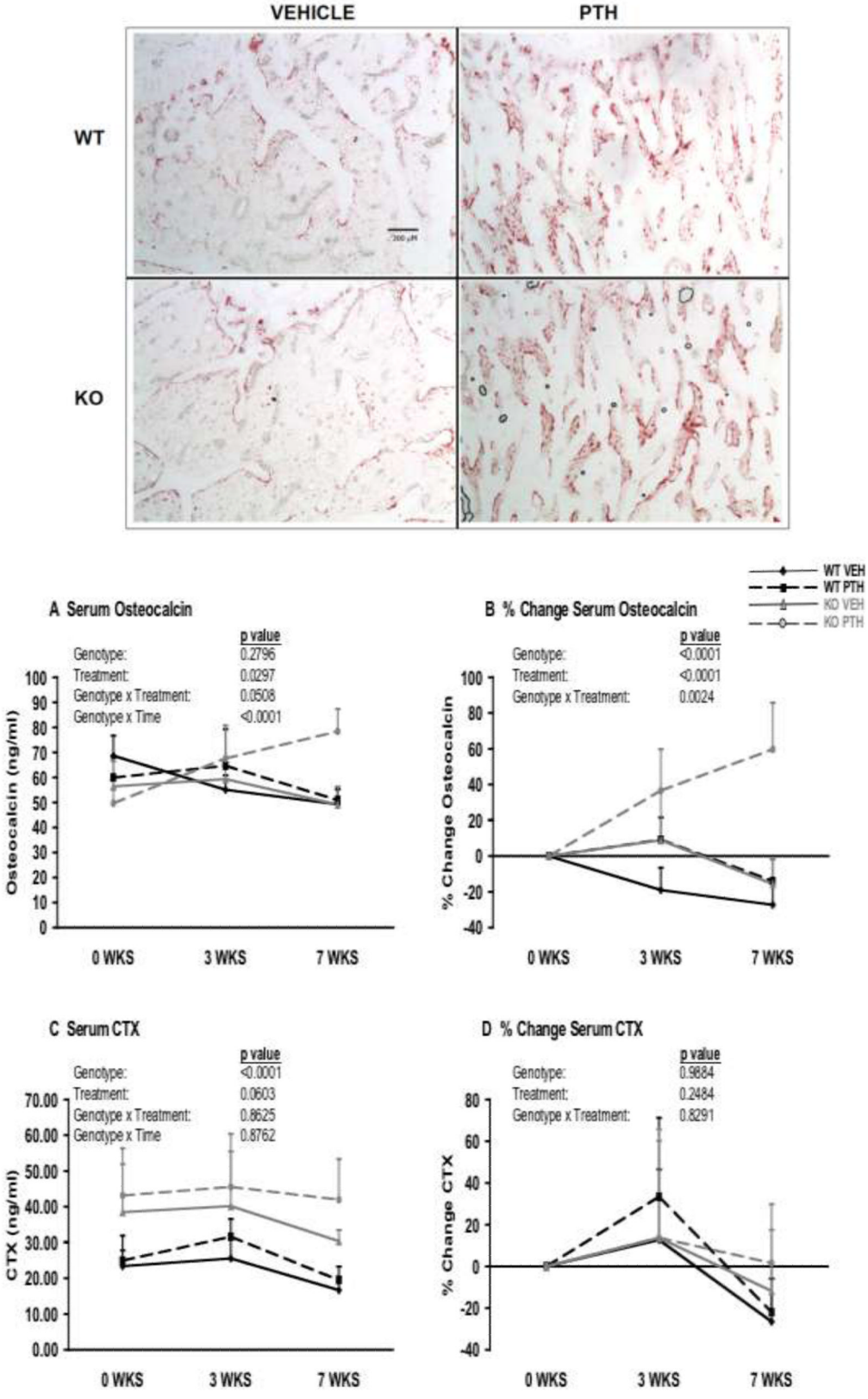

**Figure 4.**

PTH-treated *Nmp4*-KO mice exhibited strikingly distinct serum chemistries from the WT animals. Whole blood was collected and serum separated from WT and *Nmp4*-KO mice treated with intermittent PTH or vehicle (number of mice/experimental group=6–7) at baseline just prior initiation of treatment, at 3 wks of treatment, and at 7 wks of treatment. (A) The raw longitudinal serum osteocalcin concentrations showed no genotype effect, but revealed a significant treatment effect, a genotype × treatment interaction and a genotype × time interaction indicating that the WT and null mice had equivalent baseline values but that the *Nmp4*-KO had an enhanced response to hormone and a higher rate of increase over the experimental time period. (B) The % change data confirmed the raw longitudinal data revealing a significant genotype effect (higher rate of osteocalcin increase in the nulls), a treatment effect, and a genotype × treatment interaction over the experimental period. (C) The raw longitudinal serum CTX concentrations showed a genotype effect, but no significant treatment effect, no genotype × treatment interaction and no genotype × time interaction. (D) The % change CTX data showed no significant responsiveness to hormone treatment in WT and null mice. The listed p-values were determined with a repeated-measures MANOVA (longitudinal data) or a two-factor ANOVA (% change data).

**TABLE 1**

Real-time PCR primers from Assays-on-Demand™ (Applied Biosystems™, Foster City CA).

| GENE (mRNA) | | ABI Assay ID |
|---|---|---|
| *Alpl* | (Alkaline phosphatase) | Mm01187117_m1 |
| *Bcl2* | (B-cell lymphoma 2) | Mm00477631_m1 |
| *Bmp2* | (Bone morphogenic protein 2) | Mm01340178_m1 |
| *c-fms* | (Colony stimulating factor 1 receptor [CSF1R]) | Mm01266652_m1 |
| *c-fos* | (FBJ murine osteosarcoma viral oncogene homolog) | Mm00487425_m1 |
| *Col1a1* | (Type I; pro-alpha1(I) chain) | Mm00801666_g1 |
| *EphB4* | (Ephrin type-B receptor 4) | Mm01201157_m1 |
| *EphrinB2* | (EPH-related receptor tyrosine kinase ligand 5) | Mm00438670_m1 |
| *Fra-2* | (fos-related antigen 2) | Mm00484442_m1 |
| *Igf-1* | (Insulin-like growth factor 1) | Mm0043559_m1 |
| *JunD* | (Jun proto-oncogene related gene d) | Mm00495088_s1 |
| *Lef1* | (Lymphoid enhancer-binding factor-1) | Mm00550265_m1 |
| *M-csf* | (Macrophage colony stimulating factor 1) | Mm00432686_m1 |
| *Mcp-1* | (Monocyte chemotactic protein-1) | Mm00441242_m1 |
| *Mkp-1* | (MAPK phosphatase 1) | Mm00457274_g1 |
| *Mmp-13* | (Matrix metalloproteinase 13) | Mm00439491_m1 |
| *Nfatc1* | (nuclear factor of activated T-cells, cytoplasmic, calcineurin-dependent 1) | Mm012479445_m1 |
| *Nurr-1* | (Nuclear receptor-related factor 1) | Mm00443056_m1 |
| *Opg* | (Osteoprotegerin) | Mm00435452_m1 |
| *Osterix* | (Sp7 transcription factor) | Mm00504574_m1 |
| *Pthr1* | (Parathryroid hormone receptor 1) | Mm00441046_m1 |
| *Pthrp* | (Parathryoid hormone-related peptide) | Mm00436057_m1 |
| *Rage* (Ager) | (receptor for advanced glycation endproducts) | Mm00545815_m1 |
| *Rankl* | (Receptor activator for nuclear factor κ B ligand) | Mm00441908_m1 |
| *Runx2* | (Runt-related transcription factor 2) | Mm00501578_m1 |
| *Smad3* | (Sma- and Mad-related protein) | Mm01170760_m1 |
| *Sost* | (Sclerostin) | Mm00470479_m1 |

**TABLE 2A**

PTH-induced improvements in femoral trabecular architecture were equivalent in WT and *Nmp4*-KO mice, after the first 2 wks of treatment. The WT and *Nmp4*-KO mice were treated with intermittent PTH or vehcile (number of mice/experimental group=6–7) for 2 wks. A two-factor ANOVA was used to evaluate the individual parameters.

| | WT | | KO | | 2-WAY ANOVA p-values | | |
|---|---|---|---|---|---|---|---|
| | **VEH** | **PTH** | **VEH** | **PTH** | **Genotype** | **Treatment** | **Genotype × Treatment** |
| BV/TV | 0.016±0.001 | 0.042±0.012 | 0.019±0.007 | 0.047±0.017 | 0.3349 | <0.0001 | 0.8654 |
| Conn D, $mm^{-3}$ | 0.86±0.81 | 22.11±7.10 | 1.66±1.09 | 14.14±11.74 | 0.1904 | <0.0001 | 0.1131 |
| SMI | 3.39±0.21 | 2.72±0.39 | 3.51±0.25 | 3.24±0.37 | 0.0170 | 0.0009 | 0.1197 |
| Tb N, $mm^{-1}$ | 1.61±0.19 | 1.78±0.19 | 1.98±0.35 | 2.44±0.39 | 0.0002 | 0.0131 | 0.2100 |
| Tb Th, mm | 0.043±0.002 | 0.056±0.004 | 0.042±0.003 | 0.052±0.005 | 0.1232 | <0.0001 | 0.4117 |
| Tb Sp, mm | 0.629±0.066 | 0.575±0.058 | 0.523±0.103 | 0.422±0.080 | 0.3048 | 0.0004 | 0.4783 |

**TABLE 2B**

Cortical architecture at the midshaft femur from WT and *Nmp4*-KO mice treated with vehicle or intermittent PTH for 2 wks (number of mice/experimental group=7–10). The parameters include cortical area (CA, $mm^2$), marrow area (MA, $mm^2$), and total area (TA, $mm^2$) and the maximum, minimum, and polar moments of inertia ($I_{MAX}$, $I_{MIN}$, and J, respectively [$mm^4$]). A two-factor ANOVA was used to evaluate the individual parameters.

| | WT | | KO | | 2-WAY ANOVA p-values | | |
|---|---|---|---|---|---|---|---|
| | VEH | PTH | VEH | PTH | Genotype | Treatment | Genotype × Treatment |
| MA | 1.40±0.08 | 1.34±0.07 | 1.39±0.09 | 1.39±0.13 | 0.5363 | 0.4618 | 0.4141 |
| CA | 0.98±0.03 | 1.04±0.06 | 1.01±0.07 | 1.08±0.07 | 0.1073 | 0.0067 | 0.6478 |
| TA | 2.38±0.09 | 2.38±0.11 | 2.40±0.13 | 2.47±0.17 | 0.2392 | 0.4539 | 0.4223 |
| $I_{MAX}$ | 0.41±0.02 | 0.41±0.05 | 0.40±0.04 | 0.43±0.06 | 0.9661 | 0.2440 | 0.2649 |
| $I_{MIN}$ | 0.21±0.02 | 0.23±0.02 | 0.23±0.02 | 0.26±0.03 | 0.0084 | 0.0382 | 0.6726 |
| J | 0.63±0.04 | 0.64±0.07 | 0.63±0.07 | 0.69±0.09 | 0.3048 | 0.1254 | 0.3670 |

**TABLE 2C**

Values for percent change (%Δ) BMD and BMC between 8 wks and 12 wks of age. Mice were challenged with vehicle or intermittent PTH for 2 wks (10–12 wks of age; number of mice/experimental group=6–7). The listed p-values were determined with a two-factor ANOVA.

| | WT | | KO | | 2-WAY ANOVA p-values | | |
|---|---|---|---|---|---|---|---|
| | VEH | PTH | VEH | PTH | Genotype | Treatment | Genotype × Treatment |
| %ΔWB BMD | 5.27±3.02 | 10.28±2.83 | 6.18±3.61 | 9.04±2.81 | 0.8895 | 0.0032 | 0.3791 |
| %ΔWB BMC | 15.94±7.39 | 22.73±8.79 | 6.73±6.14 | 16.34±8.56 | 0.0158 | 0.0116 | 0.6410 |
| %ΔFm BMD | 12.86±4.81 | 18.49±1.69 | 8.93±4.98 | 13.84±3.74 | 0.0113 | 0.0026 | 0.8220 |
| %ΔFm BMC | 29.71±11.72 | 36.01±11.61 | 11.74±8.87 | 23.59±8.69 | 0.0009 | 0.0332 | 0.4950 |
| %ΔTb BMD | 7.25±3.48 | 14.43±4.90 | 5.98±4.73 | 8.64±4.86 | 0.0545 | 0.0096 | 0.2086 |
| %ΔTb BMC | 9.70±7.20 | 24.84±6.07 | 6.67±4.53 | 11.61±8.68 | 0.0045 | 0.0007 | 0.0608 |
| %ΔSp BMD | 6.22±7.26 | 12.93±6.41 | 9.57±11.24 | 10.99±9.44 | 0.8366 | 0.2421 | 0.4423 |
| %ΔSP BMD | 7.60±8.61 | 15.11±11.39 | 6.59±15.10 | 10.96±8.96 | 0.5635 | 0.1903 | 0.7246 |

Abbreviations: WB (whole body), FM (femur), Sp (spine).

**TABLE 2D**

Bone histomorphometry of the distal femur from WT and *Nmp4*-KO mice treated with intermittent PTH or vehicle for 7 wks (number of mice/experimental group=5–6). The parameters include mineral apposition rate (MAR), mineralizing surface/bone surface (MS/BS), bone formation rate (BFR), the TRAP-stained surface to bone surface (TRAP+ S/BS), and the number of TRAP-stained cells on the bone surface (TRAP+ N/BS). A two-factor ANOVA was used to evaluate the impact of genotype and treatment on the individual parameter. A Tukey's HSD post hoc test was used to determine differences between treatment groups if a significant genotype × treatment interaction was indicated (TRAP+ S/BS). Groups not connected by the same letter are significantly different.

| | WT | | KO | | 2-WAY ANOVA p-values | | |
|---|---|---|---|---|---|---|---|
| | **VEH** | **PTH** | **VEH** | **PTH** | **Genotype** | **Treatment** | **Gene × Treat** |
| MAR (μm/day) | 2.80±0.20 | 3.30±0.21 | 2.88±0.22 | 3.19±0.16 | 0.8288 | <0.0001 | 0.2628 |
| MS/BS (%) | 0.53±0.08 | 0.49±0.05 | 0.52±0.03 | 0.50±0.04 | 0.9331 | 0.0507 | 0.3275 |
| BFR ($\mu m^2/\mu m$/day) | 1.49±0.08 | 1.61±0.22 | 1.49±0.16 | 1.59±0.15 | 0.9135 | 0.0905 | 0.9175 |
| Trap+ S/BS [%] | 0.37±0.03 | 0.36±0.09 | 0.48±0.07 | 0.33±0.12 | 0.2420 | 0.0383 | 0.0549 |
| | | | | | | | Tukey's HSD |
| | | | | | | | KO VEH A |
| | | | | | | | WT VEH A B |
| | | | | | | | WT PTH A B |
| | | | | | | | KO PTH B |
| Trap+ N/BS [$mm^{-1}$] | 0.45±0.06 | 0.41±0.11 | 0.60±0.10 | 0.41±0.10 | 0.0863 | 0.0110 | 0.0918 |

**TABLE 3A**

Comparative femoral RNA expression of WT and *Nmp4*-KO mice treated with PTH or vehicle for 2 wks (number of mice/experimental group=6–9) or 3 wks (number of mice/experimental group=6) and harvested 1 hr after the last injection. The listed p-values were determined with a two-factor ANOVA. A Tukey's HSD post hoc test was used to determine differences between treatment groups if a significant genotype × treatment interaction was indicated. Groups not connected by the same letter are significantly different.

| GENE | WT | | KO | | 2-WAY ANOVA p-values | | | |
|---|---|---|---|---|---|---|---|---|
| | VEH | PTH | VEH | PTH | Genotype | Treatment | Gene × Treat | |
| *c-fos (2wks)* | 0.73±0.25 | 7.94±1.00 | 1.87±0.71 | 12.04±2.31 | <0.001 | <0.0001 | 0.0121 | |
| | | | | | | | Tukey's HSD | |
| | | | | | | | KO PTH | A |
| | | | | | | | WT PTH | B |
| | | | | | | | KO VEH | C |
| | | | | | | | WT VEH | C |
| *c-fos (3wks)* | 1.04±0.31 | 8.73±2.07 | 1.05±0.31 | 8.33±1.85 | 0.7380 | <0.0001 | 0.7235 | |
| *Fra-2 (2wks)* | 0.72±0.15 | 4.25±0.50 | 0.96±0.13 | 5.56±0.97 | 0.0028 | <0.0001 | 0.0301 | |
| | | | | | | | Tukey's HSD | |
| | | | | | | | KO PTH | A |
| | | | | | | | WT PTH | B |
| | | | | | | | KO VEH | C |
| | | | | | | | WT VEH | C |
| *Fra-2 (3wks)* | 1.01±0.12 | 5.32±1.23 | 1.03±0.18 | 4.72±0.98 | 0.3905 | <0.0001 | 0.3441 | |
| *Nfatc1 (2wks)* | 1.03±0.43 | 1.46±.0.31 | 1.48±0.43 | 1.96±0.27 | 0.0051 | 0.0074 | 0.8659 | |
| *Nfatc1 (3wks)* | 1.00±0.11 | 1.76±0.48 | 1.02±0.27 | 1.41±0.26 | 0.2008 | 0.0002 | 0.1699 | |
| *EphB4 (2wks)* | 0.80±0.16 | 1.27±.0.12 | 0.98±0.22 | 1.41±0.21 | 0.0466 | <0.0001 | 0.7544 | |
| *EphB4 (3wks)* | 1.01±0.16 | 1.78±0.39 | 0.95±0.33 | 1.74±0.40 | 0.7131 | <0.0001 | 0.9257 | |
| *EphrinB2 (2wks)* | 0.75±0.18 | 5.16±.0.68 | 1.19±0.27 | 5.87±1.23 | 0.0658 | <0.0001 | 0.6555 | |
| *EphrinB2 (3wks)* | 1.02±0.24 | 6.85±2.82 | 1.01±0.32 | 6.24±1.05 | 0.6209 | <0.0001 | 0.6355 | |
| *Opg (2wks)* | 0.85±0.14 | 0.82±0.14 | 1.23±0.41 | 0.97±0.21 | 0.0150 | 0.1625 | 0.2862 | |
| *Opg (3wks)* | 1.03±0.29 | 1.19±0.33 | 1.13±0.26 | 1.34±0.26 | 0.2943 | 0.1372 | 0.8389 | |
| *Rankl (2wks)* | 0.96±0.11 | 21.34±6.20 | 1.19±0.59 | 16.75±3.43 | 0.1492 | <0.0001 | 0.1124 | |
| *Rankl (3wks)* | 1.04±0.34 | 13.72±4.58 | 0.82±0.26 | 11.04±1.79 | 0.1663 | <0.0001 | 0.2367 | |
| *Rankl/Opg (2wks)* | 1.14±0.18 | 27.39±12.45 | 0.94±0.23 | 17.84±5.60 | 0.0954 | <0.0001 | 0.1092 | |

| GENE | WT | | KO | | 2-WAY ANOVA p-values | | |
|---|---|---|---|---|---|---|---|
| | VEH | PTH | VEH | PTH | Genotype | Treatment | Gene × Treat |
| *Rankl/Opg (3wks)* | 1.04±0.18 | 11.53±2.04 | 0.73±0.22 | 8.60±2.38 | 0.0207 | <0.0001 | 0.0558 |

**TABLE 3B**

Comparative femoral RNA expression of WT and *Nmp4*-KO mice treated with PTH or vehicle for 2 wks (number of mice/experimental group=6–9) and harvested 1 hr or 24 hr after the last injection. The listed p-values were determined with a two-factor ANOVA. A Tukey's HSD post hoc test was used to determine differences between treatment groups if a significant genotype × treatment interaction was indicated. Groups not connected by the same letter are significantly different.

| GENE | WT | | KO | | 2-WAY ANOVA p-values | | |
|---|---|---|---|---|---|---|---|
| | VEH | PTH | VEH | PTH | Genotype | Treatment | Gene × Treat |
| *1hr post-injection* | | | | | | | |
| *M-csf* | 1.13±0.72 | 2.14±0.70 | 1.19±0.09 | 2.87±0.53 | 0.1056 | <0.0001 | 0.1665 |
| *Mcp-1* | 0.79±0.20 | 2.60±0.90 | 0.99±0.24 | 2.61±0.70 | 0.6657 | <0.0001 | 0.7156 |
| *Bcl2* | 0.96±0.12 | 1.02±0.14 | 1.06±0.20 | 1.03±0.08 | 0.2997 | 0.7913 | 0.4563 |
| *Bax* | 1.02±0.25 | 0.91±0.14 | 0.69±0.12 | 0.71±0.04 | 0.0005 | 0.4604 | 0.3321 |
| *Nurr1* | 0.69±0.22 | 56.37±6.56 | 2.06±1.49 | 58.62±14.05 | 0.5750 | <0.0001 | 0.8914 |
| *Mkp-1* | 0.83±0.09 | 2.31±0.90 | 1.13±0.48 | 1.95±0.32 | 0.8708 | <0.0001 | 0.1022 |
| *JunD* | 0.80±0.16 | 0.94±0.16 | 0.78±0.19 | 1.10±0.16 | 0.3366 | 0.0036 | 0.2206 |
| *Smad3* | 0.78±0.12 | 1.97±0.34 | 1.05±0.26 | 2.14±0.63 | 0.1736 | <0.0001 | 0.7403 |
| *Lef1* | 0.99±0.19 | 1.52±0.30 | 1.08±0.21 | 1.36±0.27 | 0.7196 | 0.0006 | 0.2293 |
| *Rage* | 0.87±0.16 | 0.74±0.13 | 1.07±0.35 | 0.72±0.27 | 0.3655 | 0.0261 | 0.2829 |
| *24hr post-injection* | | | | | | | |
| *Runx2* | 0.86±0.21 | 1.45±0.34 | 0.59±0.23 | 1.35±0.84 | 0.2960 | 0.0007 | 0.6482 |
| *Osterix* | 0.63±0.20 | 1.61±0.48 | 0.49±0.37 | 1.67±0.96 | 0.8385 | <0.0001 | 0.6460 |
| *Col1a1* | 0.92±0.14 | 2.35±0.65 | 0.75±0.49 | 2.70±2.45 | 0.8424 | 0.0017 | 0.5964 |
| *Alpl* | 0.96±0.18 | 2.95±0.69 | 0.81±0.47 | 2.42±1.63 | 0.3286 | <0.0001 | 0.5814 |
| *Mmp13* | 0.73±0.21 | 1.05±0.28 | 0.51±0.22 | 1.23±0.61 | 0.3987 | 0.0007 | 0.3997 |
| *Sost* | 1.17±0.22 | 1.79±0.31 | 1.15±0.38 | 1.59±0.33 | 0.3328 | <0.0001 | 0.4419 |
| *Bmp2* | 1.01±0.14 | 1.41±0.24 | 0.91±0.26 | 1.15±0.39 | 0.0898 | 0.0036 | 0.4394 |
| *Pthr1* | 0.86±0.23 | 1.59±0.40 | 0.68±0.28 | 1.38±0.68 | 0.2223 | <0.0001 | 0.9071 |
| *Pthrp* | 0.75±0.18 | 1.10±0.44 | 0.89±0.44 | 1.00±0.44 | 0.9024 | 0.1154 | 0.4214 |

**TABLE 3C**

Comparative tibial RNA expression of WT and *Nmp4*-KO mice treated with PTH or vehicle for 3 wks (number of mice/experimental group=6) and harvested 1 hr after the last injection. The listed p-values were determined with a two-factor ANOVA.

| GENE | WT | | KO | | 2-WAY ANOVA p-values | | |
|---|---|---|---|---|---|---|---|
| | VEH | PTH | VEH | PTH | Genotype | Treatment | Gene × Treat |
| *c-fos* | 1.05±0.39 | 9.05±3.57 | 1.66±1.19 | 10.65±3.05 | 0.2775 | <0.0001 | 0.6243 |
| *Fra-2* | 1.02±0.23 | 4.62±1.63 | 1.28±0.31 | 7.21±3.08 | 0.0604 | <0.0001 | 0.1178 |
| *Nfatc1* | 1.02±0.20 | 1.42±0.60 | 1.36±0.45 | 2.00±0.53 | 0.0262 | 0.0136 | 0.5470 |
| *EphB4* | 1.02±0.22 | 1.80±0.75 | 1.25±0.34 | 2.07±0.34 | 0.2372 | 0.0010 | 0.9216 |
| *EphrinB2* | 1.08±0.45 | 5.13±3.31 | 1.22±0.31 | 7.40±2.19 | 0.1551 | <0.0001 | 0.2065 |
| *Opg* | 1.03±0.25 | 1.4±0.63 | 1.07±0.23 | 1.57±0.40 | 0.5314 | 0.0181 | 0.6969 |
| *Rankl* | 1.01±0.18 | 10.51±3.46 | 0.79±0.18 | 11.19±3.61 | 0.8226 | <0.0001 | 0.6618 |
| *Rankl/Opg* | 1.07±0.49 | 7.98±1.64 | 0.76±0.16 | 7.07±0.75 | 0.1248 | <0.0001 | 0.4467 |